ChemistrySelect

Full Papers
doi.org/10.1002/slct.202001656

Chemistry Europe
European Chemical Societies Publishing

Materials Science inc. Nanomaterials & Polymers

Rosehip-Extract-Assisted Green Synthesis and Characterization of Reduced Graphene Oxide

Ferda Mindivan*[a] and Meryem Göktaş[b]

Reduced-graphene oxide (RGO) is one of the main derivatives of graphene. Chemical-based techniques are used to produce large amounts of graphene in short amount of time. Hydrazine is the strong reductant but its toxic effects limit the various applications. Therefore, the usage of plants extracts has become the research interest in recent years for produced eco-friendly materials. GO was synthesized through modified Hummer's method in this study and rosehip extracts were synthesized with successful reduction reaction in different environments. The comparison of the all analysis results from RGO samples were suggested that the rosehip extract in methanol environment is very effective in obtaining RGO. EDS and BET surface results indicated that ML-RGO and MD-RGO samples which synthesis by methanol extraction, had the highest C/O ratios (4:1 and 7:1) and surface areas (230.64 and 142.85 m^2/g^{-1}), respectively as compared to other RGO samples. The ML-RGO exhibited about a 41.14% residual weight at 600 °C and had the highest thermal stability. The interlayer spacing of the diffraction peaks of MD-RGO and ML-RGO samples expanded due to a decrease of the re-stacking in graphene sheets. FESEM and HRTEM images of the MD-RGO and ML-RGO samples confirmed the flat surface with fewer layers and transparent- well exfoliated sheets. Therefore, we have validated the practicality of rosehip extract for versatile application and advocates new hopes for greener graphene.

1. Introduction

Graphene is the strongest material in existence due to its impressive physical properties, high thermal conductivity and exceptional Young's modulus.[1–2]

Graphene oxide (GO) and reduced graphene oxide (RGO) are the most important derivatives of graphene. They were synthesized by chemical conversion of graphite because this method is economical.[2–3] GO is the product of oxidation of graphene and RGO are produced through reduction reaction of GO.[1,3] The chemical reduction of GO can be performed in the presence of highly toxic and instability reducing agents, including hydrazine, di-methyl hydrazine, sodium borohydride, hydroquinone, metal hydrides.[2,4]

Recently, plant extracts such as Carrot, Grapes, Aloe-Vera, Tulsi, Custard apple, Betel, Amla etc. have offered environmentally friendly approaches to form RGO and its polymer composites, have been developed.[5] RGO is produced reducing the oxygen content of GO. It has tended to agglomerate in polymer matrix due to hydrophobic nature.[6] As such, a greener approach was initiated to improve the dispersion of RGO in polymer matrix and the interface interaction between RGO and polymer matrix and this efficient green way is still of major significance for RGO filled polymer composites.[7,3]

Ismail Z. summarized with a short review in GO reduction by 63 species plant extracts.[8] Except for the species examined in this article, Cheng et. al used urushiol extracted from the sap of lacquer trees,[7] Rattan et. al choose fresh ginger and garlic extracts[9] and also Faiz et. al preferred palm oil leaves[10] as a green reducing agent. In addition, Cuscuta reflexa leaf extract,[11] Lotus Garcinii leaf extract,[12] Euphorbia helioscopia L. leaf extract,[13] barberry fruit extract,[14] Euphorbia Wallichii leaf extract,[15] leaves of Euphorbia bungei Boiss,[16] Abutilon hirtum leaf extract[17] were used for the green synthesis of metal nanoparticles and their nanocomposites.

In the present study, rosehip extract as the green reductant was employed in the synthesis of RGO samples with the environmentally friendly procedure. The structural and thermal properties of RGO that synthesized with purchased ascorbic acid and three different rosehip extracts were investigated and compared.

2. Results and Discussion

2.1. Structure of the prepared samples

The FTIR spectrum of RGO samples is shown in Figure 1. The GO shows the hydroxyl O–H and carbonyl C=O stretching vibration, epoxy and alkoxy C–O groups peaks in the FTIR spectrum.[18] The reduction of GO with reduction agents is carried to remove the residual oxygen functional groups.[19] Mindivan and Göktas found that the intensities of the oxygen peaks in the RGO-1:1sample was lower in comparison with the

[a] Dr. F. Mindivan
Department of Bioengineering
Faculty of Engineering
Bilecik Seyh Edebali University, Bilecik, 11230, Turkey
E-mail: ferda.mindivan@bilecik.edu.tr
[b] Dr. M. Göktaş
Department of Metallurgy
Vocational College
Bilecik Seyh Edebali University, Bilecik, 11230, Turkey

Supporting information for this article is available on the WWW under https://doi.org/10.1002/slct.202001656

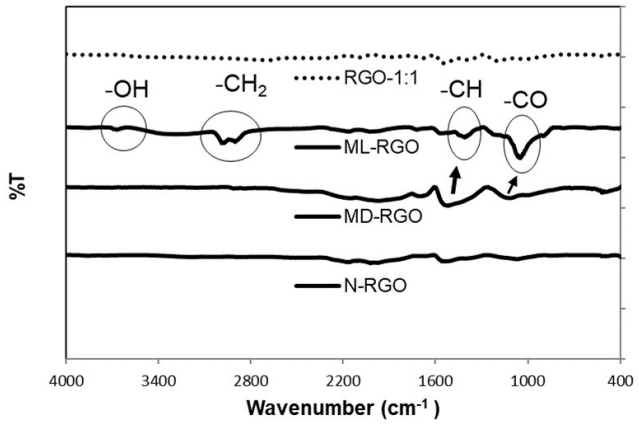

Figure 1. FTIR spectrum of RGO samples.

GO and other RGO samples.[18] This result showed reduction of GO resulted in formation of reduced graphene resembling pristine graphene.[19] In this study, the most similar sample to the RGO-1:1 sample was MD-RGO. Compared with N-RGO and ML-RGO samples, the intensities of the all FTIR peaks were obviously weakened in MD-RGO, indicating that the best reduction of GO. The obvious peaks in the ML-RGO was explained as following: 3668 cm^{-1} (the stretching vibration of -OH), 2974 and 2899 cm^{-1}(the asymmetric and symmetric stretching vibration peak of -CH_2, respectively), 1410 cm^{-1}(the in-plane bending vibration peak of -CH), 1050 cm^{-1}(the stretching vibration of CO-) proposing that liquid rosehip extract was attached to the RGO surface by a certain chemical bond.[7]

Figure 2(a) showed the XRD diffractograms of RGO samples reduced with different methods. The reported value of the diffraction peak for graphite and GO are at $2\theta^\circ = 26.4^\circ$ and 9.95° with a corresponding layer to layer distance of 0.337 nm and 0.888 nm, respectively in the literature.[20] The intense diffraction pattern seen at 9.95° and increased interlayer distance from 0.337 to 0.888 corresponds to oxygen containing functional groups in GO.[21] XRD pattern of the RGO-1:1 sample showed between $2\theta^\circ =$ 10-15° broad diffraction peak and $2\theta^\circ =$ 42.90° a sharp diffraction peak. The GO structure was disrupted by ascorbic acid that used as reduction agent for reduction reaction of RGO-1:1 sample. For the RGO samples with rosehips extract, the diffraction peak of GO completely disappeared and a broad peak at about $2\theta^\circ = 26.0^\circ$ was observed, indicating the perfect reduction and oxygen-containing groups were being lost[1,22] This new peak at $2\theta^\circ = 26.0^\circ$ was attributed to the graphene sheets.[5] Comparison of RGO samples XRD Bragg peak at $2\theta^\circ = \sim 43.0^\circ$, confirming shift in the interlayer spacing in Figure2(b). The sharp and intense diffraction peak of RGO-1:1 sample located at $2\theta^\circ = 42.90^\circ$ after reduced by ascorbic acid, this should be due to the re-stacking after reduction reaction. ML-RGO sample had the most wide peak and then the diffraction peaks of MD-RGO and N-RGO samples expanded respectively, compared to RGO-1:1. This broad peaks are also suggestive of a decrease of the re-stacking in graphene sheets.[23]

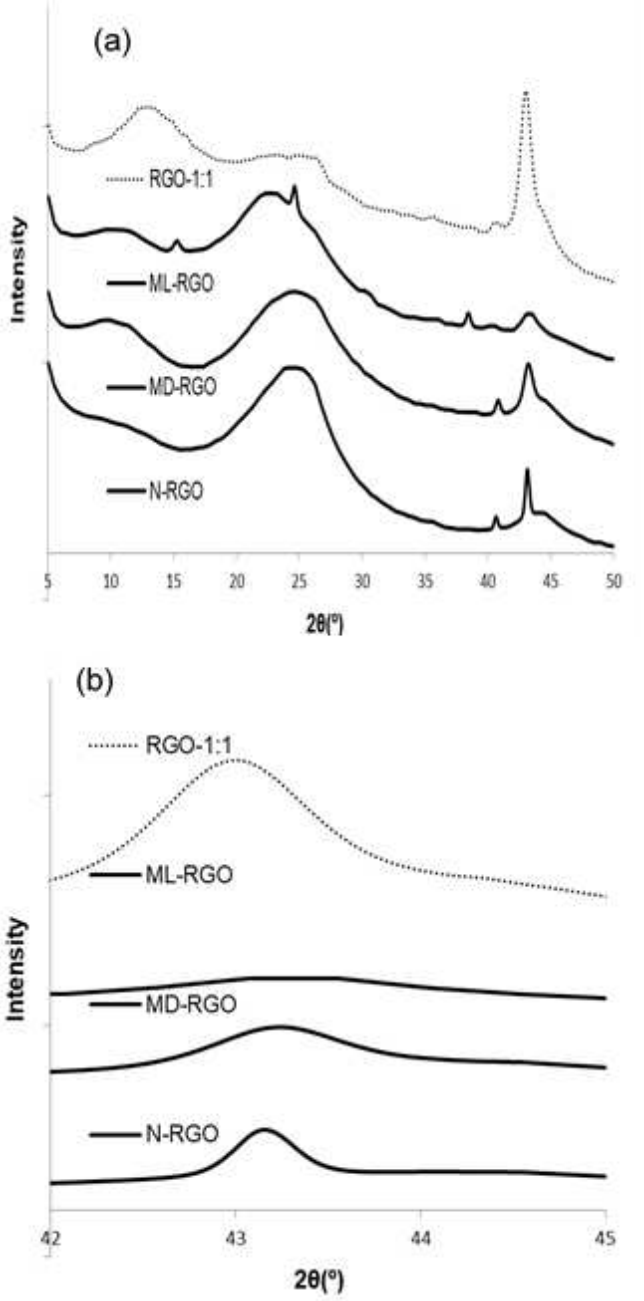

Figure 2. (a). XRD patterns of RGO samples and **(b)**. Comparison of XRD Bragg peak at $2\theta^\circ = \sim 43.0^\circ$confirming shift in the interlayer spacing.

FESEM images of the RGO samples reduced with different methods were shown in Figure 3. The FESEM images of all RGO samples showed the sheet-like morphology[24] due to a high rate of deoxygenation of GO.[8] These structures were similar with that reported for RGO samples.[25] There were crumples on the RGO-1:1 and N-RGO sheets made up of many folded layers that may be due to the self-assembly via Van der Waals' forces throughout the reduction reaction.[21–22] It is clearly seen that the surface of the ML-RGO sheets has a smooth and flat appearance. Some regions of MD-RGO sheets showed the more flat structure but some regions exhibited wrinkles layers. Jin

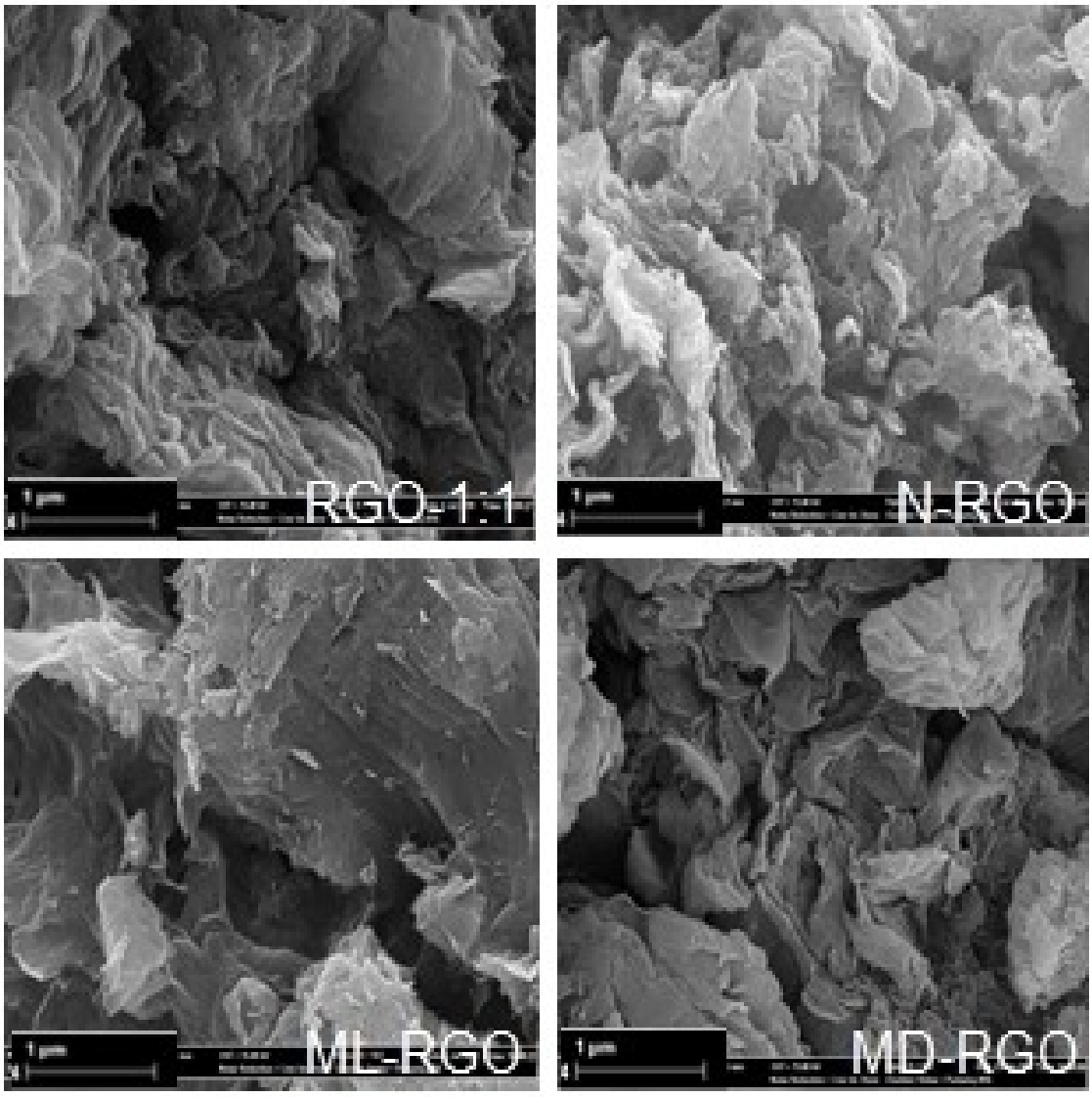

Figure 3. FESEM images of RGO samples (magnification 20.000 KX).

and co-workers experimentally examined green reduction of graphene oxide using Eucalyptus leaf extract. They have observed that there were slight wrinkles on the RGO surface since the biomolecules from Eucalyptus leaf extract dispersed well in aqueous solution.[26] Consequently, biomolecules were more homogeneously dispersed in methanol extraction than nitrogen environment.

Figure 4 was a representative HRTEM images of the RGO samples. Clearly, the RGO-1:1 and N-RGO samples owned dark areas and these areas indicated crumpled and folded layers of RGO, as given in the literature.[24] MD-RGO had black rippled morphology in a certain area but other areas showed flat surface with fewer layers.[24,27] The transparent and well exfoliated sheets of the ML-RGO were clearly observed in Figure 4. These HRTEM images of RGO samples were consistent with the FESEM surface images (Figure3). The EDS results of the RGO samples represented the amount of carbon and oxygen (wt.–%) as shown in Table 1. According to EDS results of the RGO-1:1 and RGO samples with rosehip extract, oxygen content decreased more from 27.92 atom % to 21.42, 18.76, 11.93 atom % for N-RGO, ML-RGO and MD-RGO samples (Table 1), respectively which indicated success of rosehip extract in reduction reaction. But the carbon atom content increased from 72.08% to 78.58, 81.24, 88.07% in the same order. Because biomolecules from rosehip extract were attached to the RGO surface during the reduction reaction.[26]

Results of the EDS and BET analyses were reported in Table 2. C/O value is important during the deoxygenation of GO using plant extracts for portray the efficiency of the selected plant extracts.[8] The C/O ratio of RGO-1:1 found to have improved from 2:1 to 3:1, 4:1, 7:1 for N-RGO, ML-RGO and MD-RGO samples. The surface area analysis is a critical

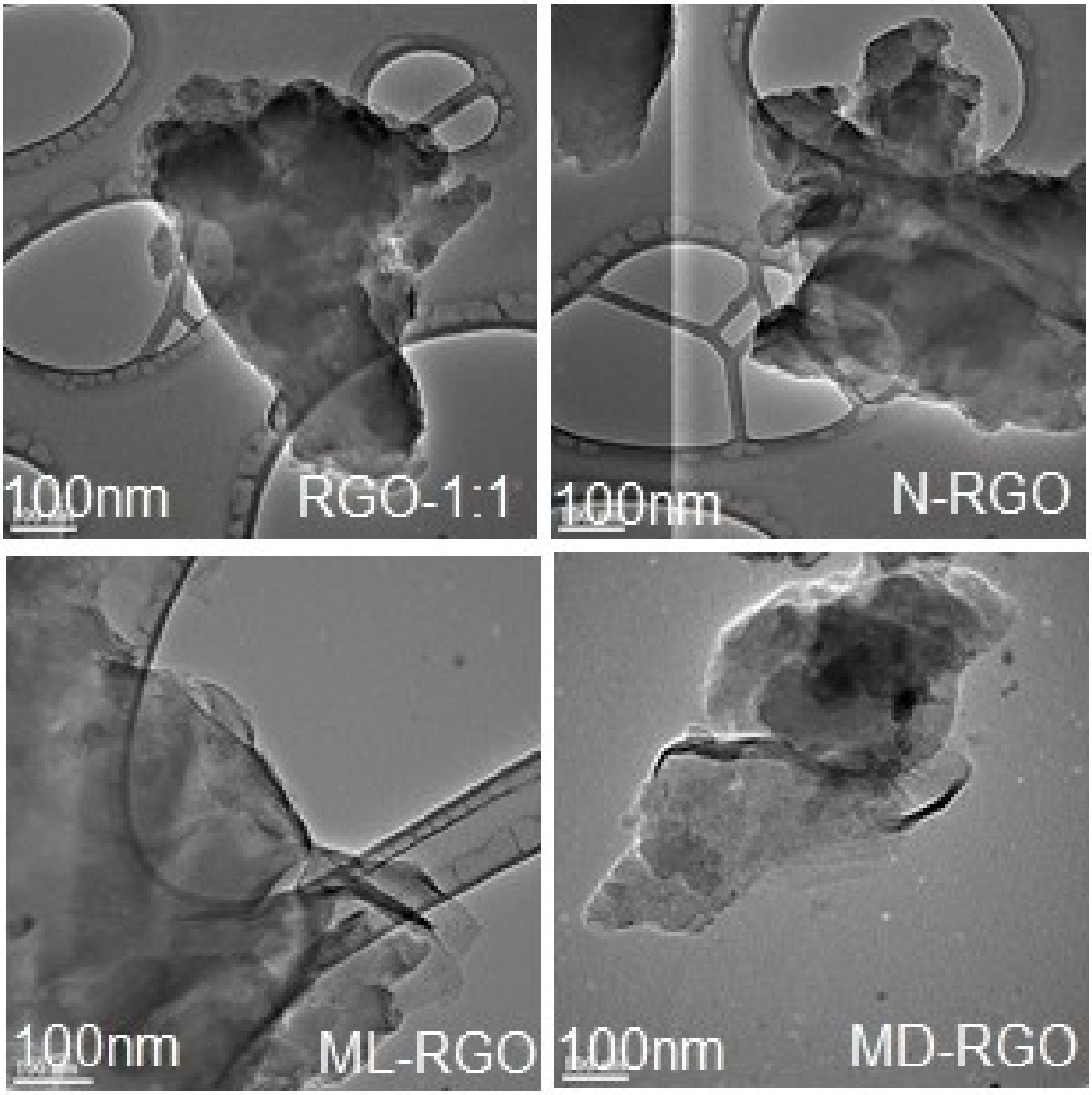

Figure 4. HRTEM images of RGO samples.

factor to obtain the potential high surface area of graphene-based materials and exploit the different application areas.[28] The lowest BET surface area of the RGO-1:1 calculated from their isotherm was 43.52 $m^2 g^{-1}$. Low BET value for RGO-1:1 sample was found because it has self-assembly and restacking phenomena as shown that XRD analysis (Figure2(a)). Compared with RGO-1:1, other RGO samples had higher BET surface area. ML-RGO had the highest BET surface area (230.64 $m^2 g^{-1}$) which was directly reflected the higher exfoliation degree of RGO.[29] And also, the same sample showed the flattest structure in the FESEM image (Figure3) compared with that of N-RGO and MD-RGO. According to this result ML-RGO sample demonstrated the most excellent dispersion.[29] BET analysis indicated that the surface areas of N-RGO and MD-RGO were determined to be 88.32 and 142.85 $m^2 g^{-1}$, respectively. MD-RGO had higher surface area than N-RGO because MD-RGO had both flat and wrinkles regions but N-RGO had completely wrinkles regions in their FESEM images (Figure3). As a result, rosehip extract especially methanol extraction inhibited agglomeration than nitrogen environment due to the strong p-p interactions between RGO layers.[30]

The thermal stability of RGO samples were examined by TGA and Figure 5 showed the TGA curves of samples. Weight loss ~ 101 °C was observed on all samples contributing to the evaporation of water.[7] For ML-RGO and MD-RGO samples, TG curve showed two steps of mass loss. The first stage of weight loss at 238 °C was about 86% and 66% of the further weight loss at about 380 °C were corresponded to the decomposition of their oxygen functional groups and the removal of more stable functional groups, respectively.[31–32] The main decomposition temperatures of N-RGO and RGO-1:1 samples were much lower (136 °C and 202 °C) than first decomposition temperatures of MD-RGO and ML-RGO. According to this result, the hydroxyl and carboxyl groups of N-RGO and RGO-1:1

Table 1. EDS results of RGO samples.

Element	Series	unn. C [wt.%]	norm. C [wt.%]	Atom. C [at.%]	Error (1 Sigma) [wt.%]
RGO-1:1					
Carbon	K-series	65.96	65.96	72.08	10.23
Oxygen	K-series	34.04	34.04	27.92	7.19
Total:		100.00	100.00	100.00	
N-RGO					
Carbon	K-series	73.37	73.37	78.58	10.51
Oxygen	K-series	26.63	26.63	21.42	5.66
Total:		100.00	100.00	100.00	
ML-RGO					
Carbon	K-series	76.47	76.47	81.24	11.53
Oxygen	K-series	23.53	23.53	18.76	5.84
Total:		100.00	100.00	100.00	
MD-RGO					
Carbon	K-series	84.71	84.71	88.07	11.27
Oxygen	K-series	15.29	15.29	11.93	3.63
Total:		100.00	100.00	100.00	

Table 2. The C/O ratios of RGO samples obtained from EDS analysis and BET surface areas of RGO samples.

Samples	C/O	$S_{BET}(m^2/g^{-1})$
RGO-1:1	2:1	43.52
N-RGO	3:1	88.32
ML-RGO	4:1	230.64
MD-RGO	7:1	142.85

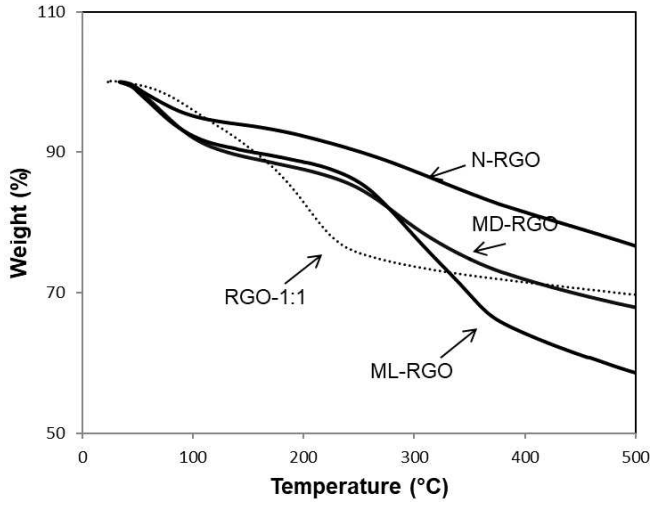

Figure 5. TGA curves of RGO samples.

samples were bonded weaker on the graphene surface. Therefore, these samples had poor thermal stability.[33] The total weight loss is about 59% for ML-RGO, 68% for MD-RGO and 70% for RGO-1:1 within the temperature of 500 °C, indicating that the hydroxyl and carboxyl groups bonded on RGO layers had been removed effectively by methanol extraction, and the ML-RGO was more stable than RGO-1:1. MD-RGO and ML-RGO had same decomposition temperatures and weight loss steps, therefore, they may be considered to have similar thermal stability although RG0-1:1 and MD-RGO showed similar % weight loss. The N-RGO displayed the least weight loss among these samples, that was, the total weight loss was only 77%.[27] The ML-RGO exhibited about a 41.14% residual weight at 600 °C indicating its excellent thermal stability than all other samples.

3. Conclusion

This study focused on the green synthesis and characterization of RGO samples by utilizing rosehip extract, a green reducing agent. The structural and thermal properties of the resulted RGO samples were characterized. The synthesis of RGO using rosehip extract revealed effective removal of oxygen-containing groups as proven by FTIR, XRD and SEM techniques. The C/O ratio have been greatly improved from 2:1 for RGO-1:1 to 7:1 for MD-RGO. The results of BET, TGA and HRTEM analysis confirm the following: firstly, the highest surface area; secondly, excellent thermal stability; and thirdly, transparent and well exfoliated sheets of the ML-RGO. As a result, rosehip extract especially methanol extraction inhibited agglomeration, reflected the higher exfoliation degree of RGO samples and decreased the re-stacking of graphene sheets than nitrogen environment. According to all results proved the efficiency of using rosehip extract as an alternative reductant agent to replace purchased ascorbic acid in the preparation.

Supporting Information Summary Paragraph

Experimental details for preparation of GO and different rosehip extract and reduction of GO by rosehip extract could be found in the Supporting Information.

Acknowledgements

The authors wish to thank Assoc. Dr. Dilek Unal from Bilecik Seyh Edebali University, Department of Molecular Biology and Genetic (Bilecik, Turkey) for her help with the preparation of Rosehip extract.

Conflict of Interest

The authors declare no conflict of interest.

Keywords: Ascorbic acid · Characterization · Graphene · Green chemistry · Rosehip extract

[1] M. Tahriri, M. Del Monico, A. Moghanian, M. Tavakkoli Yaraki, R. Torres, A. Yadegari, L. Tayebi, *Mater. Sci. Eng. C* **2019**, *102*, 171–185.
[2] B. L. Dasari, J. M. Nouri, D. Brabazon, S. Naher, *Energy* **2017**, *140*, 766–778.
[3] X. J. Lee, B. Y. Z. Hiew, K. C. Lai, L. Y. Lee, S. Gan, S. Thangalazhy-Gopakumar, S. Rigby, *J. Inst. Chem.* **2019**, *98*, 163–180.
[4] F. Mindivan, M. Göktaş, *Polym. Bull.* **2019**, *77*, 1929–1949.

[5] C. M. Kurmarayuni, S. Kurapati, S. Akhil, B. Chandu, B. M. K. Khandapu, P. R. Koya, H. B. Bollikolla, *Mater. Lett.* **2020**, *263*, 127224.
[6] V. Singh, D. Joung, L. Zhai, S. Das, S. I. Khondaker, S. Seal, *Prog. Mater. Sci.* **2011**, *56*, 1178–1271.
[7] H. Cheng, J. Lin, Y. Su, D. Chen, X. Zheng, H. Zhu, *Mater. Today Commun.* **2020**, *23*, 100938.
[8] Z. Ismail, *Ceram. Int.* **2019**, *45*, 23857–23868.
[9] S. Rattan, S. Kumar, J. K. Goswamy, *Mater. Today: Proc.* **2020**, *26*, 3327–3331.
[10] M. S. Amir Faiz, C. A. Che Azurahanim, S. A. Raba'ah, M. Z. Ruzniza, *Results Phys.* **2020**, *16*, 102954.
[11] S. Naghdi, M. Sajjadi, M. Nasrollahzadeh, K. Y. Rhee, S. M. Sajadi, B. Jaleh, *J. Inst. Chem.* **2018**, *86*, 158–173.
[12] M. Maham, M. Nasrollahzadeh, S. M. Sajadi, M. J. Colloid, *Interface Sci.* **2017**, *497*, 33–42.
[13] M. Nasrollahzadeh, M. Atarod, B. Jaleh, M. Gandomirouzbahani, *Ceram. Int.* **2016**, *42*, 8587–8596.
[14] a) M. Nasrollahzadeh, S. M. Sajadi, A. Rostami-Vartooni, M. Alizadeh, M. Bagherzadeh, *J. Colloid Interface Sci.* **2016**, *466*, 360–368;b) M. Nasrollahzadeh, M. Maham, A. Rostami-Vartooni, M. Bagherzadeh, S. M. Sajadi, *RSC Adv.* **2015**, *5*, 64769–64780.
[15] M. Atarod, M. Nasrollahzadeh, S. M. Sajadi, *RSC Adv.* **2015**, *5*, 91532–91543.
[16] M. Nasrollahzadeh, M. Atarod, S. M. Sajadi, *J. Colloid Interface Sci.* **2017**, *486*, 153–162.
[17] M. Maryami, M. Nasrollahzadeh, E. Mehdipour, S. M. Sajadi, *Int. J. Hydrogen Energy* **2016**, *41*, 21236–21245.
[18] F. Mindivan, M. Göktaş, *Mater. Test.* **19**, *61*, 1007–1011.
[19] V. Dutta, P. Singh, P. Shandilya, S. Sharma, P. Raizada, A. K. Saini, V. K. Gupta, A. Hosseini-Bandegharaei, S. Agarwal, A. Rahmani-Sani, *J. Environ. Chem. Eng.* **2019**, *7*, 103132.
[20] F. Mindivan, *Mach., Technol., Mater.* **2016**, 6, 32–35.
[21] B. Zengin Kurt, Z. Durmus, E. Sevgi, *Int. J. Hydrogen Energy* **2019**, *44*, 26322–26337.
[22] B. Haghighi, M. A. Tabrizi, *RSC Adv.* **2013**, *3*, 13365.
[23] S. Gurunathan, J. Woong Han, E. Kim, D.-N. Kwon, J.-K. Park, J.-H. Kim, *J. Nanobiotechnol.* 12, 1–16.
[24] D. Hou, Q. Liu, H. Cheng, H. Zhang, S. Wang, *J. Solid State Chem.* **2017**, *246*, 351–356.
[25] C. Bora, P. Bharali, S. Baglari, S. K. Dolui, B. K. Konwar, *Compos. Sci. Technol.* **2013**, *87*, 1–7.
[26] X. Jin, N. Li, X. Weng, C. Li, Z. Chen, *Chemosphere* **2018**, *208*, 417–424.
[27] D. Hou, Q. Liu, H. Cheng, K. Li, D. Wang, H. Zhang, *Mater. Chem. Phys.* **2016**, *183*, 76–82.
[28] R. Castaldo, G. C. Lama, P. Aprea, G. Gentile, M. Lavorgna, V. Ambrogi, P. Cerruti, *Microporous Mesoporous Mater.* **2018**, *260*, 102–115.
[29] L. Yu, L. Wang, W. Xu, L. Chen, M. Fu, J. Wu, D. Ye, *J. Environ. Sci. (Beijing, China)* **2018**, *67*, 171–178.
[30] J. Yao, S. Yao, F. Gao, L. Duan, M. Niu, J. Liu, *J. Colloid Interface Sci.* **2018**, *511*, 434–439.
[31] K. K. H. De Silva, H. H. Huang, R. K. Joshi, M. Yoshimura, *Carbon* **2017**, *119*, 190–199.
[32] H. Wang, H. Gao, M. Chen, X. Xu, X. Wang, C. Pan, J. Gao, *Appl. Surf. Sci.* **2016**, *360*, 840–848.
[33] S. Liu, H. Sun, S. Liu, S. Wang, *Chem. Eng. J. (Amsterdam, Neth.)* **2013**, *214*, 298–303.

Submitted: April 22, 2020
Accepted: July 17, 2020